

## Impacts of Organic Sorbates on the Ionic Conductivity and Nanostructure of Perfluorinated Sulfonic-Acid Ionomers

Adlai Katzenberg, Andrea Angulo, Ahmet Kusoglu,\* and Miguel A. Modestino\*



Cite This: *Macromolecules* 2021, 54, 5187–5195



Read Online

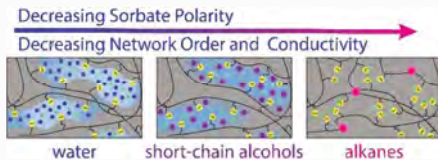
ACCESS |

Metrics & More

Article Recommendations

Supporting Information

**ABSTRACT:** This study provides insights into structure–property relationships of Nafion membranes swollen with organic sorbates, revealing correlations between sorbate polarity, ionomer domain structure, and ionic conductivity. Swelling, nanostructure, and ionic conductivity of Nafion in the presence of short-chain alcohols and alkanes were studied by infrared spectroscopy, X-ray scattering, and voltammetry. Nafion equilibrated with alkanes exhibited negligible uptake and nanoswelling, while alcohols induced nanoscopic- to macroscopic-swelling exponents that increased with alcohol polarity. In mixed-sorbate environments including organics and water, alcohols preserved the overall ionomer domain structure but altered the matrix to enable higher sorbate uptake. Alkanes did not demonstrably alter the hydrated nanostructure or conductivity. Identifying the impacts of organic sorbates on structure–property relationships in ionomers such as Nafion is imperative as membrane-based electrochemical devices find applications in emerging areas ranging from organic fuel cells to the synthesis of fuels and chemicals.



### INTRODUCTION

Perfluorinated sulfonic acid membranes (PFSAs) have enabled substantial performance enhancements and cost reductions in electrochemical energy conversion systems such as proton exchange membrane hydrogen fuel cells, redox-flow batteries, and water electrolyzers by playing a dual role as a separator and ion-conducting media that prevents crossover of chemical species between the cathodic and anodic sites while providing a low-resistance pathway for proton transport.<sup>1–3</sup> Ionic conductivity in PFSAs is intimately related to their nanostructured morphology dictated by phase separation between a hydrophobic fluoropolymer matrix and acidic side chains. This nanostructure is highly sensitive to environmental conditions; most critically, external water drives formation and hydration of acid-rich clusters that swell and percolate into an interconnected hydrated ionomer network.<sup>4</sup> The relationships between hydration, nanostructure, and key transport properties including conductivity, water transport, gas permeability, and mechanical strength in PFSAs have been investigated rigorously for decades and are highly relevant for the aqueous electrochemical systems in which they have historically been employed.<sup>1,5,6</sup>

The advantages afforded by ionomer membranes in hydrogen fuel cells and water electrolyzers have been extended to CO<sub>2</sub> electrolysis,<sup>7–10</sup> direct-methanol fuel cells (DMFCs),<sup>11–13</sup> electro-organic synthesis,<sup>14–16</sup> and electrochemical swing absorbers.<sup>17</sup> These devices expose membranes to more complex chemical environments (*i.e.*, multiple organic and inorganic chemical species) than a fuel cell or water electrolyzer, which interact with and impact the PFSA structure and transport properties. This reveals a clear need to understand structure–property relationships of ion-con-

ducting membranes in the presence of organic chemical species. Previous studies, primarily driven by the need to improve and tune performance in DMFCs, investigated the effects of ethanol and methanol on diffusion and conductivity in Nafion.<sup>18–22</sup> A number of studies have probed the ionomer structure using NMR, permeability, FTIR, and X-ray and neutron scattering.<sup>23–30</sup> Some studies also investigated and modeled how the interactions between the ion form and alcohol solution influence membrane properties.<sup>29,31–33</sup> However, as most of the studies focused on one alcohol or a specific transport property, the understanding of structure–swelling–conductivity relationships with a wider range of sorbates of varying polarities is limited. With the emergence of new technologies employing ionomers in chemically rich environments, it is even more pertinent to elucidate their impact on ionomers' local environment and transport functionality.

This study explores the effects of organic sorbates ranging from polar alcohols to nonpolar alkanes on the swelling, ionomer nanostructure and ionic conductivity of Nafion membranes. The results reveal that both macroscopic and nanoscopic swelling are strongly dependent on sorbate polarity, with a large but poorly defined ionomer domain–network in alcohol-saturated Nafion leading to low ionic

Received: March 3, 2021

Revised: April 28, 2021

Published: May 19, 2021



ACS Publications

© 2021 American Chemical Society

conductivity despite high sorbate uptake. These changes in the ionomer phase separation persist with the introduction of water in the presence of organic sorbates, leading to unique sorbate—structure—property relationships that differ from the well-understood water—Nafion relationships. The insights of this study will help guide the development and implementation of ionomers for emerging organic electrochemical devices.

## RESULTS AND DISCUSSION

Ion transport in Nafion emerges due to complex multiscale physicochemical interactions between water and the fluoropolymer. In hydrated Nafion, water solvates sulfonic acid groups, dissociating protons as mobile charge carriers. The shape and distribution of the ionomer domains within the phase-separated domain-network are determined by a balance between water sorption in the hydrophilic regions opposed by deformation of the fluoropolymer matrix during swelling.<sup>1,34</sup> Macroscopic PFSA conductivity is highly sensitive to water content as both the morphology of ionomer domains and the concentration/mobility of ions within those domains are linked to hydration levels. Both of these factors are expected to change when Nafion is swollen with organic species; size and polarity of the sorbing species have been shown to impact bulk swelling (and likely the ionomer domain structure)<sup>20,23,29,35–37</sup> and the polarity,  $pK_a$ , and viscosity would impact the concentration and mobility of protons.<sup>3,38,39</sup>

Figure 1 shows the ionic conductivity of the Nafion membrane vapor-equilibrated with water (black squares),

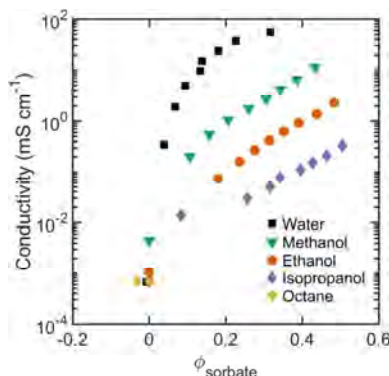


**Figure 1.** Conductivity ( $\text{mS cm}^{-1}$ ) of Nafion at room temperature equilibrated with water (black squares), alcohols (methanol, ethanol, and isopropanol; teal triangles, orange circles, and purple diamonds, respectively), and octane (yellow hexagons) from the vapor phase. Conductivity scaled not only with sorbate volume fraction but with polarity and molar volume of sorbate.

methanol (teal triangles), ethanol (orange circles), isopropanol (purple diamonds), and octane (yellow hexagons) from the vapor phase. Water- and alcohol-equilibrated Nafion conductivity values are consistent with previously reported values.<sup>31,40</sup> For all alcohols, Nafion showed nonlinear scaling of ionic conductivity with increasing concentration of sorbate in the vapor phase, a trend consistent with the impact of water uptake on PFSA ionic conductivity. On the other hand, Nafion showed minimal sorbate uptake and negligible ionic conductivity when exposed to vapor of nonpolar alkanes (see Table S1 in the Supporting Information for uptake data). For the alcohols studied, the maximum sorbate volume fraction ( $\phi_{\max}$ ) increased with decreasing sorbate polarity ( $\phi_{\max, \text{water}} < \phi_{\max, \text{EtOH}} < \phi_{\max, \text{iPrOH}}$ ), opposite to the molar sorbate uptake (Table S1, Supporting Information). This is consistent with prior literature<sup>20,30,31</sup> and attributed to the balance between solvent/solute interaction energy (more favorable for more polar species) and mechanical deformation induced by swelling, leading to small molar uptake but large volume expansion for large sorbates such as isopropanol. Alcohols can also plasticize the fluoropolymer matrix, enabling higher swelling ratios than water-swollen membranes.<sup>27,29</sup>

Conductivity at a given sorbate volume fraction, however, scaled with sorbate polarity ( $\kappa_{\text{water}} > \kappa_{\text{MeOH}} > \kappa_{\text{EtOH}} > \kappa_{\text{iPrOH}}$ ). This is consistent with consideration of each solute as a mobile electrolyte phase within the ionomer domains, with conductivity given by  $\kappa = nFC_{\text{H}^+}\mu_{\text{H}^+}$  where  $n$  is the charge of a proton,  $F$  is Faraday's constant,  $C_{\text{H}^+}$  is the proton concentration, and  $\mu_{\text{H}^+}$  is the proton mobility. Saito *et al.* demonstrated that  $\mu_{\text{H}^+}$  is the dominant factor in determining the ionomer ionic conductivity and decreased logarithmically with the alkyl chain length for Nafion swollen with alcohols.<sup>29</sup> This was attributed to the increased contribution from the Grotthuss proton-hopping mechanism in the presence of smaller alcohol molecules. However, this scaling is complicated by morphological considerations in PFSAs where sorbate uptake plays a critical role in the percolation of ion-conducting domains and where for a given sorbate, the PFSA ionic conductivity generally increases with the volume fraction of the mobile phase.

The decreasing conductivity of Nafion with increased sorbate volume fraction could be attributed to the interplay of the mobility and concentration of protons in each of these sorbates as well as distinct changes in the ionomer morphology when swollen with alcohols rather than water. In general, hydrated Nafion exhibits a morphology characterized by locally flat and highly branched water-rich domains embedded in a fluoropolymer matrix.<sup>4,41–44</sup> This morphology has been widely studied by small-angle X-ray scattering (SAXS), which reveals a broad scattering peak attributed to water-rich domains around scattering vector  $q$  of  $0.15 \text{ \AA}^{-1}$  or domain spacing ( $d_{\text{space}} = 2\pi/q$ ) between 3 and 6 nm.<sup>45–51</sup> Figure 2 shows Nafion's SAXS profiles under ambient environments and equilibrated with liquid water, methanol, ethanol, isopropanol, hexane, heptane, and octane. Alkanes induced minimal change in the scattering

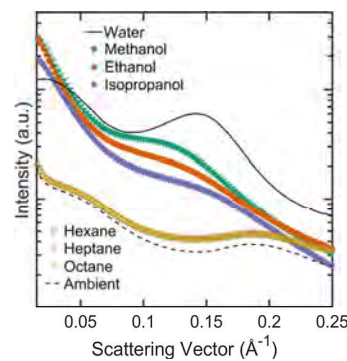


**Figure 2.** (a) SAXS profiles of Nafion 117 equilibrated with various liquid sorbates. Alkanes induced little change in the scattering profiles, consistent with their minimal mass uptake. Alcohols induced a strong shift in the ionomer peak to lower scattering vectors while increasing its breadth and decreasing its intensity relative to water-equilibrated Nafion. Profiles offset for clarity.

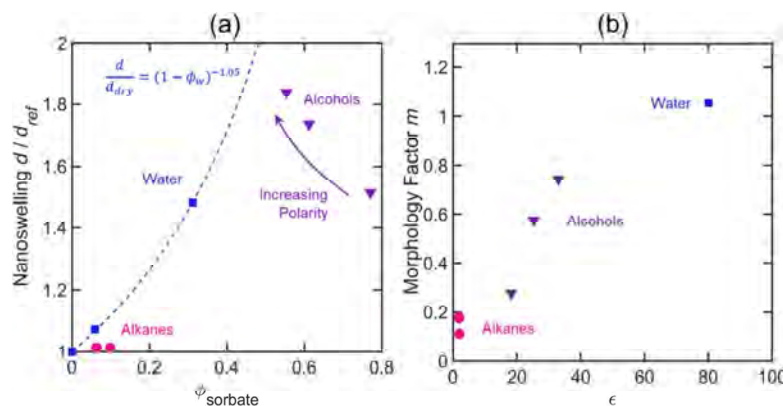


**Figure 3.** (a) Nanoswelling/macrosopic swelling relationships for Nafion swollen with organic species deviated significantly from water-swollen Nafion. The dashed line shows experimental data fitted to eq 2, with  $m = 1.05$ . (b) Nanoscale morphology factor  $m$  increased monotonically with sorbate dielectric constant.

profiles, consistent with their negligible bulk uptake. Alcohol-swollen Nafion, however, exhibited significant changes in the scattering behavior; the ionomer peak shifted to lower  $q$  values relative to the ambient-equilibrated material, indicating ionomer domain swelling, but with broader peaks than water-swollen Nafion. There was also a clear shift to larger  $q$  (smaller  $d_{space}$ ) with increasing alcohol size. While alkane-saturated Nafion showed similar  $d_{space}$  and full width at half-maximum (fwhm) to the ambient-equilibrated material, these features scaled with sorbate polarity in the case of alcohol-saturated Nafion; increasing polarity coincided with increased  $d_{space}$  and lower fwhm (see Figure S4 in the Supporting Information). Less polar alcohols result in smaller ionomer nano-domains within a network of increasing spatial disorder, contributing to the reduction in ionic conductivity despite high alcohol volume fraction. It is also important to note that the matrix knee ( $q \sim 0.05 \text{ \AA}^{-1}$ ), arising from the ordered distribution of PTFE crystallites within the fluoropolymer matrix, is absent in the alcohol-swollen Nafion (Figure 2). Alcohols, while interacting more preferably with the fluoropolymer matrix compared to water, are still not able to dissolve PTFE crystallites, so this loss of scattering is likely due to redistribution (*i.e.*, increasing isotropy) of crystallites within the ionomer's amorphous matrix, which is consistent with observations in acetone-swollen Nafion<sup>23</sup> and with matrix plasticization observed in methanol- and isopropanol-swollen Nafion.<sup>24,27,30</sup> Young *et al.* also reported changes to the intercrystalline morphology of Nafion swollen with ethanol, including quenching of the intercrystalline peak at a high sorbate volume fraction.<sup>30</sup>

Changes in nanostructure morphology are also clear when comparing the ionomer nano-domain swelling ( $d_{saturated}/d_{ref}$ ) to bulk swelling for the different species (Figure 3a). Nafion exhibits a well-established correlation between nanoswelling and water volume fraction

$$\frac{d}{d_{ref}} = (1 - \Delta\phi_s)^{-m} = (1 + \Delta\phi_p)^{-m} \quad (1)$$

where subscript ref denotes a selected reference state,  $\Delta\phi_s$  is the change in volume fraction of sorbate,  $\Delta\phi_p$  is the change in volume fraction of polymer between reference states, and  $m$  is a constant that indicates the topology/morphology of ionomer domains.<sup>1,34</sup> Typically, for water-swollen Nafion, fully dehy-

drated Nafion is chosen as the reference state, such that eq 1 simplifies to

$$\frac{d}{d_{dry}} = (1 - \phi_{water})^{-m} = \phi_p^{-m} \quad (2)$$

For Nafion swollen with water ( $\phi_p > 0.5$ ),  $m$  is slightly greater than 1, indicating a locally lamellar domain structure with mesoscale connectivity, while in dispersion ( $\phi_p < 0.5$ ),  $m$  approaches 0.5, reflecting cylindrical polymer aggregates.<sup>41,45,52,53</sup> Figure 3a shows that organic sorbates deviated significantly from water-Nafion behavior with nanoswelling related to sorbate polarity. Alkanes induced almost no nanoswelling in Nafion, confirming the limited penetration of nonpolar sorbates into ionomer domains. Alcohols did cause substantial nanoswelling in Nafion, with magnitude decreasing monotonically with increasing sorbate volume fraction (*i.e.*, methanol > ethanol > isopropanol). This indicates that the distribution of sorbate within the ionomer structure is impacted by sorbate chemical identity, as in the absence of structural changes, the nanoswelling would scale identically with sorbate volume fraction regardless of the sorbate identity. Figure 3b shows that the morphological exponent  $m$  was strongly correlated to sorbate polarity (represented as the dielectric constant) and shifted toward lower values (indicating loss of lamellar structure and transition toward dispersion-like scaling) with decreasing polarity. It should be noted that the  $m$  values reported here are based only on dry, ambient, and sorbate-saturated Nafion. Without intermediate swelling fractions, the relationship in eq 1 cannot be precisely determined. Still, the trend clearly shows a correlation between sorbate polarity and the relationship between the bulk and nano-domain swelling through morphological rearrangements.

These changes likely arise from the affinity of the sorbate for different moieties in the polymer; highly polar water molecules ( $\epsilon \sim 80$ ) strongly solvate sulfonic acid moieties but display minimal affinity for perfluoroether side chains, resulting in a strong phase separation and a relatively sharp fluoropolymer–water interface. Alcohols and acetone have been shown to interact with the perfluoroether side chains, partition across the water–fluoropolymer interface, and impact the fluoropolymer matrix.<sup>22–24,27–30,54</sup> The implications of this modified water–fluoropolymer interface on the structure and transport are qualitatively similar to changes incurred by the cation partitioning processes, which alter the ionic character and

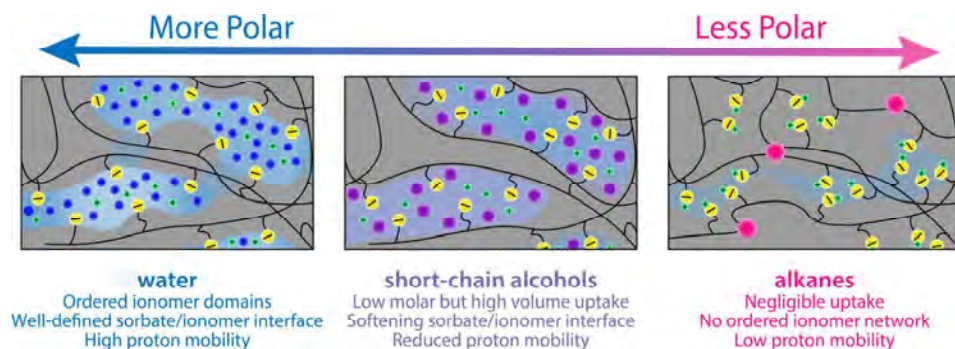


**Figure 4.** Overview of the proposed impacts of sorbate polarity on the ionomer structure and transport. Water strongly solvates protons and sulfonic acid groups while displaying minimal affinity for perfluoroether side chains or the fluoropolymer backbone. This produces a sharp fluoropolymer–ionomer interface with a high concentration of mobile protons. Alcohols of increasing size (decreasing polarity) increasingly mix with perfluoroether side chains, softening the fluoropolymer–sorbate interface and decreasing proton mobility due in part to increases in local viscosity. Alkanes display minimal affinity for ionic groups and the fluoropolymer and do not significantly alter Nafion from its dry state.

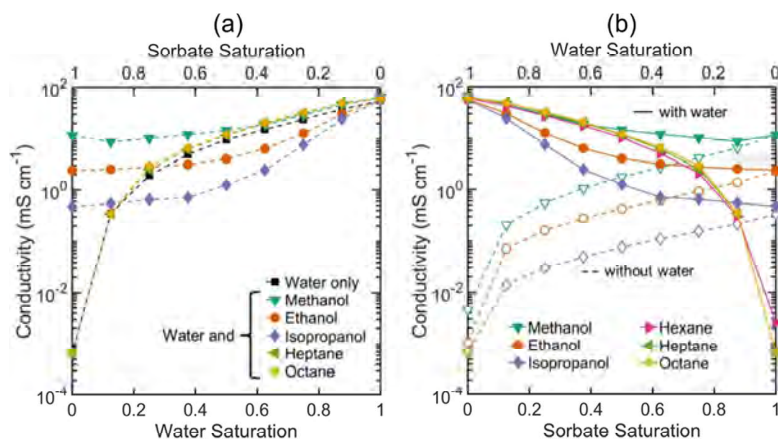


**Figure 5.** (a) Ionic conductivity of Nafion swollen with water vapor alone (black squares) and with various organic species in the vapor phase. While nonpolar alkanes had minimal impact on the ionic conductivity, alcohols imparted high conductivity at low water saturation (high organic saturation) but approached the conductivity of water-swollen Nafion at higher water saturation (low organic saturation). (b) Ionic conductivity of Nafion swollen with organics alone (empty markers) and organic vapor balanced with water vapor (filled markers). Ionic conductivities of alcohol- and water-swollen Nafion were generally between that of the individual sorbate cases, indicating the uptake and influence of both species on the ionomer conductivity.

local environment.<sup>1,30,38,39,55–58</sup> In the case of organic sorbates, however, the extent of these interfacial modulations changes significantly with the sorbate type and polarity, with broad implications for domain–network morphology. Increased mixing of the sorbate and fluoropolymer would have the following impacts on ionomer domain structure and conductivity summarized in Figure 4: (i) reduced phase separation and redistribution of sorbate across the liquid–fluoropolymer interface, (ii) significant changes in the shape and ordering of ionomer domains accompanied by disruption of the domain–network, and (iii) increased penetration of the fluoropolymer into swollen ionomer channels. Together, these effects would result in increased network tortuosity (per structural changes), increased local viscosity within ionomer channels, and decreased H<sup>+</sup> mobility despite a higher fraction of the mobile phase.

While studying the properties of PFSAs in pure sorbate environments is useful in characterizing sorbate–ionomer interactions, organic electrochemical devices commonly employ water as a solvent to maintain membrane hydration,<sup>59</sup> and thus it is important to understand how organic species interact with PFSAs in the presence of water.

The limited uptake of alkanes by Nafion in pure-sorbate studies suggests that a mixture of alkane and water vapor will likely lead to similar nano-swellings and ionic conductivity to pure water, while alcohol–water mixtures may exhibit more complex behavior. At a given water saturation, adding alcohol vapor may add mechanical resistance to hydration by further deforming the fluoropolymer matrix, shifting the equilibrium toward a lower water concentration. However, these mechanical considerations are complicated by the possible alcohol-induced matrix plasticization and change in domain–network morphology. To assess these competing effects, Nafion was exposed to controlled mixtures of water and organic vapor. In these experiments, a water-saturated stream was balanced by an organic vapor-saturated stream. Figure 5a shows the impact of introduction of organic vapors at a given water saturation on Nafion's conductivity. As expected, alkanes did not significantly impact the water uptake or ionic conductivity of water-swollen Nafion since their penetration was negligible.

Alcohols induced large polarity-related differences in Nafion ionic conductivity at low water contents, which became progressively smaller as the water content increased,

approaching the water-saturated ionic conductivity. At a low water content, the presence of alcohols increased Nafion's ionic conductivity due to the inherent conductivity of alcohol-swollen Nafion, but this improvement was lost at intermediate and high water saturation. Alcohol-driven loss of conductivity at intermediate water content scaled similarly to pure sorbate systems ( $\kappa_{\text{water}} \sim \kappa_{\text{Water+MeOH}} > \kappa_{\text{Water+EtOH}} > \kappa_{\text{Water+iPrOH}}$ ), which suggests appreciable uptake of these alcohols in addition to water. Figure 5b shows the ionic conductivity of Nafion swollen with organic vapor alone (empty markers) and organic vapor balanced with water vapor (filled markers). It is clear that at intermediate alcohol–water saturation, the conductivity generally fell between that of the pure sorbates (water and alcohol), suggesting both species are absorbed and contribute to the ionic conductivity. In these environments, ion conduction is governed by the same physical considerations as in single-sorbate environments (*i.e.*, the shape and tortuosity of ionomer domains and the mobility and concentration of protons within those domains). Similar observations were recently reported for cation-exchanged PFSI; controlled Cerium ion doping was shown to impact ionomer conductivity by reducing proton concentration and mobility as well as increasing tortuosity of the overall domain structure.<sup>38</sup> Mixed ionomer–sorbate systems may exhibit additional complexity due to the unknown composition of the sorbate mixture inside the ionomer domains.

The sorbate mixture composition was quantitatively determined by ATR–FTIR using a linear regression trained with water-saturated and organic-saturated Nafion FTIR spectra to determine the relative contributions of each sorbate. Figure 6 shows the sorbate uptake isotherms of alcohol in

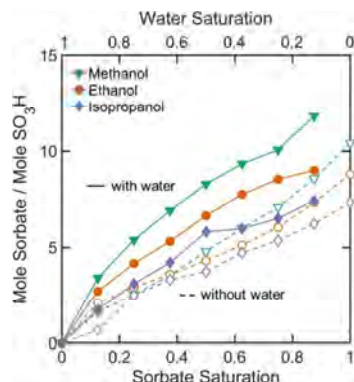


**Figure 6.** Molar uptake of organic sorbates with water (filled markers, solid lines) and without water (empty markers, dashed lines) determined by regression of ATR–FTIR spectra. Overall, mixed-sorbate systems with alcohol exhibited higher molar uptake than single-sorbate systems, with much of the increase attributed to additional alcohol uptake.

Nafion in mixed- and single-sorbate environments, with consistently higher alcohol uptake in Nafion with the presence of water. This was previously reported for Nafion equilibrated with methanol and water and shown to be thermodynamically consistent with equations derived from the Gibbs energy.<sup>22</sup> This complementary behavior points to differences in how the chemical species interact with and swell Nafion; swelling in Nafion at a given water activity is generally constrained by the fluoropolymer resistance to mechanical deformation. As observed in pure-sorbate environments, alcohols may interact

with the perfluoroether chains and soften the water–fluoropolymer interface while reducing the matrix stress and allowing for higher total sorbate uptake than in a single-sorbate environment at the same chemical activity. Alcohols can benefit from this by mixing with water in the ionomer regions and by partitioning across the water–fluoropolymer interface. This would result in increased total swelling and possibly a non-uniform distribution of alcohol and water within the ionomer domain structure. This possible distribution of sorbates is also consistent with ionic conductivity results for mixed-sorbate Nafion, which show conductivity higher than alcohol alone as water contributes to increased proton mobility and produces a stronger phase-separation of ionomer domains. On the other hand, mixed-sorbate-swollen Nafion conductivity was lower than water-swollen Nafion as alcohols in the ionomer domains increase the local viscosity and their partitioning across the water–fluoropolymer interface would alter the domain structure and increase the side chain penetration into the water-rich domains.

The impacts of mixed-sorbate environments on Nafion's phase-separated nanomorphology were investigated by SAXS of Nafion equilibrated with mixed vapor saturated with water and an organic species. SAXS profiles are shown in Figure 7

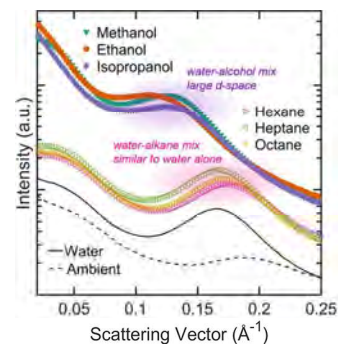


**Figure 7.** SAXS profiles of Nafion equilibrated with saturated water vapor and saturated methanol (teal triangles), ethanol (orange circles), isopropanol (purple diamonds), hexane (pink right arrows), heptane (green left arrows), and octane (yellow hexagons) vapor. Profiles of Nafion ambient (dashed line) and equilibrated with water vapor (solid line) are included for reference. Profiles offset for clarity.

and reveal a well-defined ionomer peak with alkane–water mixtures closely resembling the spectra of water-equilibrated Nafion. Negligible uptake of alkanes resulted in a similar Nafion nanostructure, swelling, and conductivity to Nafion with water alone. Alcohol–water mixtures show that an ionomer peak shifted to lower scattering vector  $q$  (larger domain spacing) than water alone and with greater intensity/sharpness than alcohol alone. Increased total sorbate uptake for mixed sorbate systems is expected to produce larger domain spacing, so this does not necessarily indicate a change in the way water–alcohol are partitioned as was observed in the pure sorbates (*i.e.*, no change in  $m$  can be resolved). However, the matrix knee is notably absent from isopropanol/water- and ethanol/water Nafion, suggesting the role of the alcohol in altering the distribution of crystallites in pure sorbates persists in the presence of water. SAXS profiles suggest that mixed water–alcohol environments preserve the overall domain structure of water-swollen Nafion but with larger interdomain spacing enabled by matrix plasticization, disruption of intercrystalline order, and/or distribution of alcohol across the

water–fluoropolymer interface. Water appears to play a critical role in ionomer network formation, confirming the orders-of-magnitude increase in Nafion ionic conductivity at a given organic saturation upon introduction of water (Figure 5b).

## CONCLUSIONS

The findings presented here show that the well-established hydration–structure–property relationships are fundamentally different in Nafion membranes when swollen with organic sorbates. In organic-swollen Nafion, the sorbate polarity plays a key role in determining the bulk swelling and ionomer domain structure likely based on the solvation tendencies of the sorbate toward the fluoropolymer. In general, more polar sorbates produced larger ionomer domains at lower sorbate contents and yielded a higher-conductivity ionomer. In the presence of water and organic species, water played a crucial role in the ionomer network formation while alcohols may have aided bulk and ionomer-domain swelling by penetrating across the fluoropolymer–water interface. Alkanes showed almost no sorption and therefore minimal impact on ionic conductivity or domain structure regardless of the water content. These results point to fundamental physical relationships between sorbate polarity, ionomer nanostructure, and key ionomer performance metrics, which may limit the applicability of PFSAs for electrochemical systems employing alcohols and other polar organic species while also providing guidance for the design of different ionomer–sorbate systems for applications involving electro-organic reactions.

## MATERIALS

Nafion 117 and Nafion D2021 were purchased from The Fuel Cell Store (College Station, TX). All other chemicals were purchased from Sigma-Aldrich, Inc. (St. Louis, MO).

## EXPERIMENTAL SECTION

Concise experimental information is included here. A full expanded description of all experimental procedures and calculations can be found in the *Supporting Information*.

For ionic conductivity and sorbate uptake experiments, sorbate saturation was controlled by mixing dry and sorbate-saturated nitrogen streams at controlled flow rates. The sorbate-saturated stream was generated by flowing nitrogen through a midget impinger bubbler (Ace Glass) filled with the species of interest. The sorbate saturation  $s_A$  can be approximated as

$$s_A = \frac{\dot{v}_a}{\dot{v}_a + \dot{v}_0} \quad (3)$$

where  $\dot{v}_a$  and  $\dot{v}_0$  are the flow rates of sorbate-saturated and dry nitrogen, respectively. The total flow rate was maintained at 200 sccm. For the mixed sorbate (*i.e.*, organic and water) experiments, the nitrogen stream was replaced with a water-saturated stream and saturation of each species was determined as described above, assuming no interaction between sorbates in the vapor phase.

**Sorbate Uptake.** ATR–FTIR spectra were collected with a Nicolet 6700 FTIR spectrometer from Thermo Scientific with the Smart iTR attachment and the ZnSe single-pass crystal (Thermo Electron North America, West Palm Beach, FL) as the average of 50 spectra collected from 650 to 4000  $\text{cm}^{-1}$ . After background collection under nitrogen flow, Nafion films were drop-cast on the crystal from Nafion 2021 to produce a film with thickness  $>200 \mu\text{m}$ , much greater than the expected light penetration depth into Nafion (on the order of 1  $\mu\text{m}$ , dependent on the light wavelength and Nafion refractive index). After drying films at ambient conditions for 30 min and under vacuum for 2 h, residual alcohol was detected in the ATR–FTIR spectra that persisted under vacuum and/or nitrogen flow. This

residual alcohol was fully removed by rehydrating the films with deionized water for 20 min and then drying again under vacuum. After the final drying step, the ATR crystal was loaded into the FTIR in a custom-built PTFE cell with the flow inlet and outlet. At each saturation setpoint, ATR–FTIR spectra were collected periodically until the difference in absorption at a given wavenumber deviated by less than 1% over a 30 min interval. Plotted points represent final measured values.

Sorbate uptake at intermediate (between 0 and 1) vapor saturation was estimated by linear regression of the as-saturated Nafion ATR–FTIR spectrum to the dry and fully saturated spectra. Relative uptake of sorbate A ( $X_A$ ) was defined as the dependent variable and the measured absorbance at each wavenumber  $A_j$ , where subscript  $j$  is the index for each wavenumber, as the independent variable. 12,238 wavenumbers were evaluated in the range 3600 to 650  $\text{cm}^{-1}$ . Relative sorbate uptake  $X_A$  was defined as

$$X_A = a + \sum_{j=1}^{12,238} b_j A_j \quad (4)$$

where  $b_j$  is a weighted fitting parameter describing the sensitivity of  $A_j$  to sorbate A saturation at the  $j$ th wavenumber, and  $a$  is an additional fitting parameter. Mass fraction of sorbate in the ionomer was calculated as

$$m_A = X_A \left( \frac{\Delta M}{M_{\text{dry}} + \Delta M} \right) \quad (5)$$

where  $m_A$  is the mass fraction of species A and  $M_{\text{dry}}$  and  $\Delta M$  are the initial (dry) mass and mass uptake of sorbate, respectively, determined by gravimetric dynamic vapor sorption. This method offers several key advantages over traditional absorbance-based analysis techniques (*i.e.* Beer's Law at a fixed wavenumber or linear combination of the absorbance spectra of individual components) as it (i) accounts for changes in Nafion and sorbate spectra upon mixing, (ii) uses the entire absorbance range, and (iii) enables simple analysis of multi-sorbate mixtures. In cases with multiple sorbates, a multi-target linear regression was performed using the spectra of dry Nafion and Nafion saturated with each sorbate. Relative uptake  $X_i$  of each sorbate was estimated as

$$X_i = a_i + \sum_{j=1}^{12,238} b_{ij} A_j \quad (6)$$

where subscript  $i$  denotes the sorbate. The linear regression was performed using Scikit-learn in Python.<sup>60</sup> Demonstration of ATR–FTIR and regression results for methanol-equilibrated Nafion can be found in the *Supporting Information*, and regression software is publicly available online.<sup>61</sup>

**Ionic Conductivity.** Nafion ionic conductivity was measured using a BT-110 four probe in-plane membrane conductivity clamp (Scribner Associates, Inc., Southern Pines, NC). A strip of Nafion 117 was cut to a width of  $\sim 1 \text{ cm}$  and long enough to completely cover two platinum-gauze force leads (2.5 cm). Membrane width was measured from photographs of the membrane in ImageJ by length-calibrated pixel count, with at least 20 measurements per membrane. Dry thickness of Nafion 117 is reported as  $183 \mu\text{m}$  and was verified by micrometer measurement prior to affixing the conductivity clamp. The conductivity clamp was placed in a vented environmental chamber with the flow inlet.

Sorbate saturation was incremented from 0 to 1 in steps of 0.125. The membrane was equilibrated at each step for 2 h or until the difference in resistance values deviated by less than 0.1% over a 10 min interval. Mixed-sorbate experiments were started at full organic saturation (water saturation of 0) and the organic saturation was decremented as the water saturation was incremented.

Conductivity was determined by linear-sweep voltammetry from  $-0.1$  to  $0.1 \text{ V}$  at a sweep rate of  $20 \text{ mV s}^{-1}$ . Cell resistance  $R$  was determined from the slope of the LSV trace and conductivity was calculated as

$$\kappa = \frac{L}{Rwt} \quad (7)$$

where  $L$  is the distance between the counter- and working-sense leads,  $R$  is the cell resistance, and  $w$  and  $t$  are the width and thickness of the dry membrane scaled by the linear swelling  $\epsilon$  at the given saturation step

$$\epsilon = s_A \left( 1 + \frac{\Delta V}{V_{\text{dry}}} \right)^{1/3} \quad (8)$$

where  $\Delta V/V_{\text{dry}}$  is the volumetric expansion of Nafion 117 saturated with sorbate A as determined by ATR-FTIR regression at the same saturation. Conductivity was measured every 10 min during vapor equilibration until the deviation between measurements was less than 0.1%.

**Small Angle X-ray Scattering.** SAXS measurements were performed at beamline 7.3.3 of the Advanced Light Source at Lawrence Berkeley National Lab. The X-ray energy was 10 keV with a monochromator resolution  $E/dE$  of 100. Scattering patterns were acquired with a 2D Dectris Pilatus 1M CCD area detector ( $172 \mu\text{m} \times 172 \mu\text{m}$  pixel size). The scattering wave vector,  $q = 4\pi \sin\left(\frac{\theta}{2}\right)/\lambda$ , where  $\theta$  is the scattering angle, was in the range of  $0.004\text{--}0.4 \text{ \AA}^{-1}$ . Experiments were conducted *in situ* by equilibrating the membrane samples in liquid or in vapor using custom-designed sealed sample holders with X-ray transparent Kapton windows for imaging. For liquid-equilibrated experiments, circular membrane samples were completely immersed in the holder filled with liquid (water or alcohol). Vapor-equilibration of the samples was accomplished using sealed holders containing a controlled mixture of water and sorbate in the solution reservoir. For each equilibrium method, samples were equilibrated for at least 2 h and SAXS images for vapor- and liquid-equilibrated samples were collected *in situ* with an exposure time of 20 s. The collected two-dimensional scattering patterns were azimuthally integrated to generate 1-D intensity profiles,  $I(q)$ , which were corrected for background scattering. From the SAXS data, hydrophilic-domain spacing and fwhm were calculated using a Gaussian fit to the ionomer scattering peak. Because Nafion samples were not thoroughly dried before sorbate exposure, they should be considered ambient-equilibrated, suggesting the appropriate reference state for nanoswelling calculations is impacted by residual water. For polar sorbates (water and alcohol), the small amount of residual water can be expected to desorb and become diluted in the much larger liquid reservoir, making dry Nafion the appropriate reference state. In nonpolar sorbates, ambient Nafion is the appropriate reference state as the alkane liquid reservoir would have minimal interactions with water absorbed in the ionomer domains of Nafion.

## ASSOCIATED CONTENT

### Supporting Information

The Supporting Information is available free of charge at <https://pubs.acs.org/doi/10.1021/acs.macromol.1c00494>.

Sorbate mass, molar, and volume uptake; ATR-FTIR spectra collection; ATR-FTIR spectral regression; and SAXS ([PDF](#))

## AUTHOR INFORMATION

### Corresponding Authors

Ahmet Kusoglu — Lawrence Berkeley National Laboratory, Berkeley, California 94720, United States;  [orcid.org/0000-0002-2761-1050](https://orcid.org/0000-0002-2761-1050); Email: [akusoglu@lbl.gov](mailto:akusoglu@lbl.gov)

Miguel A. Modestino — Tandon School of Engineering, New York University, Brooklyn, New York 11201, United States;  [orcid.org/0000-0003-2100-7335](https://orcid.org/0000-0003-2100-7335); Email: [modestino@nyu.edu](mailto:modestino@nyu.edu)

## Authors

Adlai Katzenberg — Tandon School of Engineering, New York University, Brooklyn, New York 11201, United States; Present Address: Lawrence Berkeley National Laboratory, Berkeley, CA 94720, United States;  [orcid.org/0000-0002-4793-5853](https://orcid.org/0000-0002-4793-5853)

Andrea Angulo — Tandon School of Engineering, New York University, Brooklyn, New York 11201, United States

Complete contact information is available at: <https://pubs.acs.org/10.1021/acs.macromol.1c00494>

## Notes

The authors declare no competing financial interest.

## ACKNOWLEDGMENTS

A.K. acknowledges the funding from the U.S. Department of Energy Hydrogen and Fuel Cell Technologies Office (HFTO) (Contract no. DE-AC02-05CH11231). This work also made use of facilities at the Advanced Light Source Beamline 7.3.3, supported by the Office of Science, Office of Basic Energy Sciences, of the U.S. Department of Energy (Contract no. DE-AC02-05CH11231). The authors would like to acknowledge the financial support of the National Science Foundation and NYU Tandon School of Engineering through the M.A.M. startup fund. This material is based upon work supported by the National Science Foundation under grant no. 1943972.

## REFERENCES

- (1) Kusoglu, A.; Weber, A. Z. New Insights into Perfluorinated Sulfonic-Acid Ionomers. *Chem. Rev.* **2017**, *117*, 987–1104.
- (2) Ayers, K.; Danilovic, N.; Ouimet, R.; Carmo, M.; Pivovar, B.; Bornstein, M. Perspectives on Low-Temperature Electrolysis and Potential for Renewable Hydrogen at Scale. *Annu. Rev. Chem. Biomol. Eng.* **2019**, *10*, 219–239.
- (3) Kushner, D. I.; Crothers, A. R.; Kusoglu, A.; Weber, A. Z. Transport Phenomena in Flow Battery Ion-Conducting Membranes. *Curr. Opin. Electrochem.* **2020**, *21*, 132–139.
- (4) Allen, F. I.; Comolli, L. R.; Kusoglu, A.; Modestino, M. A.; Minor, A. M.; Weber, A. Z. Morphology of Hydrated As-Cast Nafion Revealed through Cryo Electron Tomography. *ACS Macro Lett.* **2015**, *4*, 1–5.
- (5) Grot, W. Discovery and Development of Nafion Perfluorinated Membranes. *Chem. Ind.* **1985**, 647–649.
- (6) Grot, W. G. Polymerization of Fluorinated Copolymers. U.S. Patent 5,281,680 A, 1994.
- (7) Higgins, D.; Hahn, C.; Jaramillo, T. F.; Weber, A. Z.; Xiang, C. Gas-Diffusion Electrodes for Carbon Dioxide Reduction: A New Paradigm. *ACS Energy Lett.* **2019**, *4*, 317–324.
- (8) Pătru, A.; Binniger, T.; Pribyl, B.; Schmidt, T. J. Design Principles of Bipolar Electrochemical Co-Electrolysis Cells for Efficient Reduction of Carbon Dioxide from Gas Phase at Low Temperature. *J. Electrochem. Soc.* **2019**, *166*, F34–F43.
- (9) Weekes, D. M.; Salvatore, D. A.; Reyes, A.; Huang, A.; Berlinguette, C. P. Electrolytic CO<sub>2</sub> Reduction in a Flow Cell. *Acc. Chem. Res.* **2018**, *51*, 910–918.
- (10) Verma, S.; Lu, S.; Kenis, P. J. A. Co-Electrolysis of CO<sub>2</sub> and Glycerol as a Pathway to Carbon Chemicals with Improved Technoeconomics Due to Low Electricity Consumption. *Nat. Energy* **2019**, *4*, 466–474.
- (11) Wasmus, S.; Küver, A. Methanol Oxidation and Direct Methanol Fuel Cells: A Selective Review. *J. Electroanal. Chem.* **1999**, *461*, 14–31.
- (12) Neburchilov, V.; Martin, J.; Wang, H.; Zhang, J. A Review of Polymer Electrolyte Membranes for Direct Methanol Fuel Cells. *J. Power Sources* **2007**, *169*, 221–238.

(13) Jörissen, L.; Gogel, V.; Kerres, J.; Garche, J. New Membranes for Direct Methanol Fuel Cells. *J. Power Sources* **2002**, *105*, 267–273.

(14) Blanco, D. E.; Prasad, P. A.; Dunningan, K.; Modestino, M. A. Insights into Membrane-Separated Organic Electrosynthesis: The Case of Adiponitrile Electrochemical Production. *React. Chem. Eng.* **2020**, *5*, 136–144.

(15) Jing, Y.; Wu, M.; Wong, A. A.; Fell, E. M.; Jin, S.; Pollack, D. A.; Kerr, E. F.; Gordon, R. G.; Aziz, M. J. In Situ Electrosynthesis of Anthraquinone Electrolytes in Aqueous Flow Batteries. *Green Chem.* **2020**, *22*, 6084–6092.

(16) Pletcher, D.; Green, R. A.; Brown, R. C. D. Flow Electrolysis Cells for the Synthetic Organic Chemistry. *Chem. Rev.* **2018**, *118*, 4573–4591.

(17) Voskian, S.; Hatton, T. A. Faradaic Electro-Swing Reactive Adsorption for CO<sub>2</sub> Capture. *Energy Environ. Sci.* **2019**, *12*, 3530–3547.

(18) Hallberg, F.; Vernersson, T.; Pettersson, E. T.; Dvinskikh, S. V.; Lindbergh, G.; Furó, I. Electrokinetic Transport of Water and Methanol in Nafion Membranes as Observed by NMR Spectroscopy. *Electrochim. Acta* **2010**, *55*, 3542–3549.

(19) Beckingham, B. S.; Lynd, N. A.; Miller, D. J. Monitoring Multicomponent Transport Using In Situ ATR FTIR Spectroscopy. *J. Membr. Sci.* **2018**, *550*, 348–356.

(20) Zhao, Q.; Carro, N.; Ryu, H. Y.; Benziger, J. Sorption and Transport of Methanol and Ethanol in H<sup>+</sup>-Nafion. *Polymer* **2012**, *53*, 1267–1276.

(21) Hallinan, D. T.; Elabd, Y. A. Diffusion and Sorption of Methanol and Water in Nafion Using Time-Resolved Fourier Transform Infrared–Attenuated Total Reflectance Spectroscopy. *J. Phys. Chem. B* **2007**, *111*, 13221–13230.

(22) Gates, C. M.; Newman, J. Equilibrium and Diffusion of Methanol and Water in a Nafion 117 Membrane. *AIChE J.* **2000**, *46*, 2076–2085.

(23) Berens, S. J.; Yahya, A.; Fang, J.; Angelopoulos, A.; Nickels, J. D.; Vasenkov, S. Transition between Different Diffusion Regimes and Its Relationship with Structural Properties in Nafion by High Field Diffusion NMR in Combination with Small-Angle X-ray and Neutron Scattering. *J. Phys. Chem. B* **2020**, *124*, 8943–8950.

(24) Shi, C.; Liu, T.; Chen, W.; Cui, F.; Liu, L.; Cai, Y.; Li, Y. Interaction, Structure and Tensile Property of Swollen Nafion® Membranes. *Polymer* **2021**, *213*, 123224.

(25) Feng, K.; Tang, B.; Wu, P. A Self-Protection Phenomenon in the Nafion Membrane When It Breathes in Methanol-Saturated Air. *Phys. Chem. Chem. Phys.* **2016**, *18*, 19440–19450.

(26) Soniat, M.; Houle, F. A. Swelling and Diffusion during Methanol Sorption into Hydrated Nafion. *J. Phys. Chem. B* **2018**, *122*, 8255–8268.

(27) Jung, B.; Moon, H.-M.; Baroña, G. N. B. Effect of Methanol on Plasticization and Transport Properties of a Perfluorosulfonic Ion-Exchange Membrane. *J. Power Sources* **2011**, *196*, 1880–1885.

(28) Rivin, D.; Kendrick, C. E.; Gibson, P. W.; Schneider, N. S. Solubility and Transport Behavior of Water and Alcohols in Nafion. *Polymer* **2001**, *42*, 623–635.

(29) Saito, M.; Tsuzuki, S.; Hayamizu, K.; Okada, T. Alcohol and Proton Transport in Perfluorinated Ionomer Membranes for Fuel Cells. *J. Phys. Chem. B* **2006**, *110*, 24410–24417.

(30) Young, S. K.; Trevino, S. F.; Beck Tan, N. C. Small-Angle Neutron Scattering Investigation of Structural Changes in Nafion Membranes Induced by Swelling with Various Solvents. *J. Polym. Sci., Part B: Polym. Phys.* **2002**, *40*, 387–400.

(31) Affoune, A. M.; Yamada, A.; Umeda, M. Conductivity and Surface Morphology of Nafion Membrane in Water and Alcohol Environments. *J. Power Sources* **2005**, *148*, 9–17.

(32) Tandon, R.; Pintauro, P. N. Solvent Effects during Multi-component Ion Uptake into a Nafion Cation-Exchange Membrane. *J. Membr. Sci.* **2009**, *341*, 21–29.

(33) Godino, M. P.; Barragán, V. M.; Izquierdo-Gil, M. A.; Villaluenga, J. P. G.; Seoane, B.; Ruiz-Bauzá, C. Methanol-Water Solution Transport in Nafion Membranes with Different Cationic Forms. *Sep. Sci. Technol.* **2011**, *46*, 944–949.

(34) Kusoglu, A.; Savagatrup, S.; Clark, K. T.; Weber, A. Z. Role of Mechanical Factors in Controlling the Structure-Function Relationship of PFSA Ionomers. *Macromolecules* **2012**, *45*, 7467–7476.

(35) Randová, A.; Bartovská, L.; Hovorka, Š.; Friess, K.; Izák, P. The Membranes (Nafion and LDPE) in Binary Liquid Mixtures Benzene + Methanol - Sorption and Swelling. *Eur. Polym. J.* **2009**, *45*, 2895–2901.

(36) Welch, C.; Labouriau, A.; Hjelm, R.; Orler, B.; Johnston, C.; Kim, Y. S. Nafion in Dilute Solvent Systems: Dispersion or Solution? *ACS Macro Lett.* **2012**, *1*, 1403–1407.

(37) Abroshan, H.; Akbarzadeh, H.; Taherkhani, F.; Parsafar, G. Effect of Water – Methanol Content on the Structure of Nafion in the Sandwich Model and Solvent Dynamics in Nano-Channels; a Molecular Dynamics Study. *Mol. Phys.* **2011**, *109*, 709.

(38) Baker, A. M.; Crothers, A. R.; Chintam, K.; Luo, X.; Weber, A. Z.; Borup, R. L.; Kusoglu, A. Morphology and Transport of Multivalent Cation-Exchanged Ionomer Membranes Using Perfluorosulfonic Acid–CeZ<sup>+</sup> as a Model System. *ACS Appl. Polym. Mater.* **2020**, *2*, 3642–3656.

(39) Crothers, A. R.; Darling, R. M.; Kusoglu, A.; Radke, C. J.; Weber, A. Z. Theory of Multicomponent Phenomena in Cation-Exchange Membranes: Part II. Transport Model and Validation. *J. Electrochem. Soc.* **2020**, *167*, 013548.

(40) Liu, L.; Chen, W.; Li, Y. An Overview of the Proton Conductivity of Nafion Membranes through a Statistical Analysis. *J. Membr. Sci.* **2016**, *504*, 1–9.

(41) Kreuer, K.-D.; Portale, G. A Critical Revision of the Nano-Morphology of Proton Conducting Ionomers and Polyelectrolytes for Fuel Cell Applications. *Adv. Funct. Mater.* **2013**, *23*, 5390–5397.

(42) Hickner, M. A. Water-Mediated Transport in Ion-Containing Polymers. *J. Polym. Sci., Part B: Polym. Phys.* **2012**, *50*, 9–20.

(43) Rollet, A.-L.; Diat, O.; Gebel, G. A New Insight into Nafion Structure. *J. Phys. Chem. B* **2002**, *106*, 3033–3036.

(44) Schmidt-Rohr, K.; Chen, Q. Parallel Cylindrical Water Nanochannels in Nafion Fuel-Cell Membranes. *Nat. Mater.* **2008**, *7*, 75–83.

(45) Gierke, T. D.; Munn, G. E.; Wilson, F. C. The Morphology in Nafion Perfluorinated Membrane Products, as Determined by Wide- and Small-Angle x-Ray Studies. *J. Polym. Sci., Polym. Phys. Ed.* **1981**, *19*, 1687–1704.

(46) Hsu, W. Y.; Gierke, T. D. Ion Transport and Clustering in Nafion Perfluorinated Membranes. *J. Membr. Sci.* **1983**, *13*, 307–326.

(47) Gebel, G.; Lambard, J. Small-Angle Scattering Study of Water-Swollen Perfluorinated Ionomer Membranes. *Macromolecules* **1997**, *30*, 7914–7920.

(48) Kusoglu, A.; Modestino, M. A.; Hexemer, A.; Segalman, R. A.; Weber, A. Z. Subsecond Morphological Changes in Nafion during Water Uptake Detected by Small-Angle X-Ray Scattering. *ACS Macro Lett.* **2012**, *1*, 33–36.

(49) Roche, E. J.; Pineri, M.; Duplessix, R. Phase Separation in Perfluorosulfonate Ionomer Membranes. *J. Polym. Sci., Part A-2* **1982**, *20*, 107–116.

(50) Fujimura, M.; Hashimoto, T.; Kawai, H. Small-Angle X-Ray Scattering Study of Perfluorinated Ionomer Membranes. 2. Models for Ionic Scattering Maximum. *Macromolecules* **1982**, *15*, 136–144.

(51) Su, G. M.; Cordova, I. A.; Yandrasits, M. A.; Lindell, M.; Feng, J.; Wang, C.; Kusoglu, A. Chemical and Morphological Origins of Improved Ion Conductivity in Perfluoro Ionene Chain Extended Ionomers. *J. Am. Chem. Soc.* **2019**, *141*, 13547–13561.

(52) Berrod, Q.; Lyonnard, S.; Guillermo, A.; Ollivier, J.; Frick, B.; Manseri, A.; Améduri, B.; Gébel, G. Nanostructure and Transport Properties of Proton Conducting Self-Assembled Perfluorinated Surfactants: A Bottom-Up Approach toward PFSA Fuel Cell Membranes. *Macromolecules* **2015**, *48*, 6166–6176.

(53) Loppinet, B.; Gebel, G.; Williams, C. E. Small-Angle Scattering Study of Perfluorosulfonated Ionomer Solutions. *J. Phys. Chem. B* **1997**, *101*, 1884–1892.

(54) Gebel, G.; Aldebert, P.; Pineri, M. Swelling Study of Perfluorosulphonated Ionomer Membranes. *Polymer* **1993**, *34*, 333–339.

(55) Shi, S.; Weber, A. Z.; Kusoglu, A. Structure-Transport Relationship of Perfluorosulfonic-Acid Membranes in Different Cationic Forms. *Electrochim. Acta* **2016**, *220*, 517–528.

(56) Shi, S.; Liu, Z.; Lin, Q.; Chen, X.; Kusoglu, A. Role of Ionic Interactions in the Deformation and Fracture Behavior of Perfluorosulfonic-Acid Membranes. *Soft Matter* **2020**, *16*, 1653–1667.

(57) Yeager, H. L.; Steck, A. Cation and Water Diffusion in Nafion Ion Exchange Membranes: Influence of Polymer Structure. *J. Electrochem. Soc.* **1981**, *128*, 1880–1884.

(58) Münchinger, A.; Kreuer, K.-D. Selective Ion Transport through Hydrated Cation and Anion Exchange Membranes I. The Effect of Specific Interactions. *J. Membr. Sci.* **2019**, *592*, 117372.

(59) Blanco, D. E.; Modestino, M. A. Organic Electrosynthesis for Sustainable Chemical Manufacturing. *Trends Chem.* **2019**, *1*, 8–10.

(60) Pedregosa, F.; Varoquaux, G.; Gramfort, A.; Michel, V.; Thirion, B.; Grisel, O.; Blondel, M.; Prettenhofer, P.; Weiss, R.; Dubourg, V.; et al. Scikit-Learn: Machine Learning in Python. *J. Mach. Learn. Res.* **2011**, *12*, 2825–2830.

(61) Angulo, A. Organic-Sorbates-on-Ionic-Conductivity-and-Nano-structure-of-Perfluorinated-Sulfonic-Acid-Ionomers. *Github Repository*, 2021.